



**HAL**  
open science

## Friction noise model for two beams in contact

Bernard Laulagnet

► **To cite this version:**

Bernard Laulagnet. Friction noise model for two beams in contact. 18th International Congress on Sound & Vibration, Jul 2011, Rio de Janeiro, Brazil. page 124. hal-00609457

**HAL Id: hal-00609457**

**<https://hal.science/hal-00609457>**

Submitted on 19 Jul 2011

**HAL** is a multi-disciplinary open access archive for the deposit and dissemination of scientific research documents, whether they are published or not. The documents may come from teaching and research institutions in France or abroad, or from public or private research centers.

L'archive ouverte pluridisciplinaire **HAL**, est destinée au dépôt et à la diffusion de documents scientifiques de niveau recherche, publiés ou non, émanant des établissements d'enseignement et de recherche français ou étrangers, des laboratoires publics ou privés.

# FRICION NOISE MODEL FOR TWO BEAMS IN CONTACT

Bernard Laulagnet

*Vibration Acoustics Laboratory, National Institute of Applied Sciences of Lyon, 20 bis avenue J. Capelle 69621 Villeurbanne cedex, France.*

*e-mail: [bernard.laulagnet@insa-lyon.fr](mailto:bernard.laulagnet@insa-lyon.fr)*

Instabilities generated by friction are responsible for many noises in real life, such as squealing, squeak or juddering. The challenge to model this strongly non-linear acoustic radiation problem depends on the possibility to predict the interacting contact forces with accuracy, since they entirely govern the sound radiation and the way this sound is perceived as, squeak, squeal or juddering. A first approach to tackle this problem consists in linearising it and to calculate a solution around a sliding equilibrium. The main advantage is the simplicity of this approach which consists in calculating the perturbed solution which will exhibit, if the system is unstable, complex solutions. We only have the possibility to detect instabilities, but we are in the impossibility to describe what happens during the instability and for example separating juddering from squealing. A second approach consists in finding the entire solution solving the problem in time. This second approach is used here, in the case of two interacting beams; one is pushed on the other at rest, by external constant forces or driven at constant velocity. The equations of movement of the two beams are solved explicitly in time. A Coulomb friction law is introduced in the equations of the contact point taking into account all the possible status: separated, sliding or sticking. Solutions for the contact force, contact point trajectories and acceleration contact point are calculated at each instant of time for durations of one or two seconds, allowing acoustic radiation simulations. We show how different events appear depending on the beam relative angle, friction coefficient, and how instability occurs leading to limit cycles appearance.

---

## 1. Introduction

In the real life, friction noise contributes highly to the city surrounding and namely squealing or juddering is common during breaking phases of metros or trains arriving in station. These situations are most of the time related to instabilities involved in the contact area. The contact forces are responsible for the vibrations of the bodies interacting and consequently of the noise radiated. From the acoustical point of view, the main difficulty consists in building a model able to predict the contact force reasonably, since the time behaviour of this latter will highly influence the time patterns of the sound radiated. Namely sound radiation patterns can be completely different for a system said instable, and the perceived sound can be concentrated in the high frequency range (squealing) or in a different manner (juddering). These reasons lead us to tackle this problem in time (see reference <sup>1-2</sup>). For the contact force we use a Coulomb law with a friction constant coefficient independent of the velocity.

The aim of this paper is to present the modelisation of two beams in a friction contact, to point out the vibrations phenomena involved at the contact point. The same modelisation can be extended for a beam interacting with a plate, which in turn will radiate in the surrounding fluid. For the sake of brevity, this acoustical part of the modelisation will not be presented here and do not represent

the heart of the problem and the main difficulty too. The attention is here focussed on the results issued of the use of the Coulomb law in this interacting beam friction problem and what is the dynamic beam behaviours induced. It is shown that under a critical coefficient the system is stable and that above, instabilities occurs leading to squealing or juddering.

## 2.Presentation of the beam contact problem

We show in the figure 1, the system of two beams separated initially by a gap  $e$ . The beam 1 is pushed by a constant external force  $F$  at its extremity  $A$  along its principal axis, and will enter in contact with the beam 2 at rest.  $E$  is the other extremity of the beam 1 and in the following the moving contact point. During simulation the relative angle between the two beams remains constant since the boundary conditions of the beam 1 is blocked in rotation but free in displacement. The other beam is simply supported at its extremities. The two beams can vibrate in flexion and longitudinally too. The contact force tangential component  $\lambda_T(t)$  and the contact force normal component  $\lambda_N(t)$  allow us to assure sliding, sticking or separated status of the contact point  $E$  and follow the coulomb friction law where  $\mu$  is the constant friction coefficient:

$$\begin{aligned}
 |\lambda_T(t)| &= \mu \lambda_N(t) : \textit{sliding} \\
 |\lambda_T(t)| &< \mu \lambda_N(t) : \textit{sticking}; \quad \lambda_N(t) = 0 : \textit{separated}; \quad \lambda_N(t) \geq 0
 \end{aligned}
 \tag{1}$$

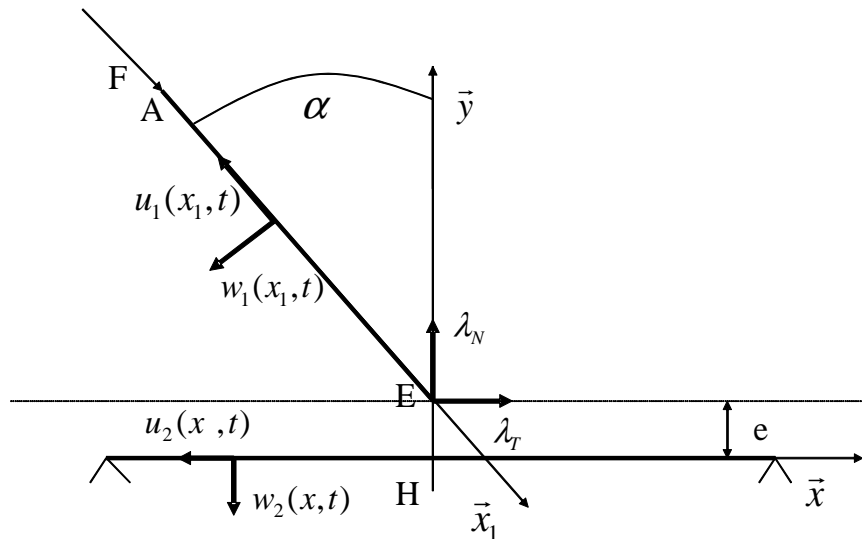


Figure 1: Synoptic view of the two interacting beams.

## 2.1 Equations of the beams interacting punctually with a dry friction

$$\rho S \ddot{u}_1(x_1, t) = ES \frac{\partial^2 u(x_1, t)}{\partial x_1^2} + [\lambda_N(t) \cos \alpha - \lambda_T(t) \sin \alpha] \delta(x_1 - x_E) \delta_C(t) \quad (2)$$

$$\rho S \ddot{w}_1(x_1, t) = -EI \frac{\partial^4 w_1(x_1, t)}{\partial x_1^4} - [\lambda_N(t) \sin \alpha + \lambda_T(t) \cos \alpha] \delta(x_1 - x_E) \delta_C(t) + F \delta(x_1 - x_A) \quad (3)$$

$$\rho S \ddot{u}_2(x, t) = ES \frac{\partial^2 u(x, t)}{\partial x^2} + \lambda_T(t) \delta(x - x_E(t)) \delta_C(t) \quad (4)$$

$$\rho S \ddot{w}_2(x, t) = -EI \frac{\partial^4 w_1(x, t)}{\partial x^4} + \lambda_N(t) \delta(x - x_E(t)) \delta_C(t) \quad (5)$$

The equations (2) and (3) are related to the longitudinal and flexural movements of the beam one and the equations (4) and (5) related to those of the beam two. For simplicity the sections  $S$  and the material characteristics ( $E$  and  $\rho$ ) are the same for the two beams, only the lengths are different.

$\delta_C(t)$  is a Kronecker symbol equal to zero when the beams are separate and equal to unity when in contact. Written like this the system of equation is valuable when beams are in contact or not since when separated the contact force vanishes. On contrary for example  $\delta(x_1 - x_A)$  denotes the Dirac distribution convenient to describe punctual forces.

## 2.2 Method of resolution

The set of equation (1-5) are then solved explicitly in time. Moreover at each instant of time the position of the beam point extremity E is calculated without the contact force. If the point E has not penetrated the beam 2, the calculation can go on. If not, a penetration occurred, meaning that the contact force must assure the continuity displacement in between E and a point  $Q(t)$  belonging to the beam 2:

$$|\lambda_T(t)| < \mu \lambda_N(t) : \text{sticking} ; \lambda_N(t) \geq 0 \text{ and}$$

$$X(E) = X(Q(t)); \quad Y(E) = Y(Q(t))$$

or

$$|\lambda_T(t)| = \mu \lambda_N(t) : \text{sliding} \quad Y(E) = Y(Q(t)) \text{ only}; \quad (6)$$

If the sticking condition is acceptable, displacement continuity constraint is fully verified in both direction. If sticking condition is not acceptable, the displacement constraint condition is verified only along the normal direction of contact, allowing a sliding movement in the tangential direction of contact. In the following the beam 1 is described using a finite element schema. On contrary, for the beam 2, the modal method is used to solve (4) and (5), using the modal basis of the beam 2, simply supported in flexion and clamped in traction at both extremities.

### 3. Numerical simulation results

#### 3.1A sliding stable case

We present in the following figures (2-3) and (4-5), a stable case where the incident angle is  $45^\circ$  and the friction coefficient is 0.5. The constant force is not applied along the principal axis of the beam 1, but perpendicular to at point A. We know that all friction coefficient under unity (smaller than  $\tan(45^\circ)$ ), lead to stable sliding movements. This is shown by the sliding trajectory of the contact point E and by the contact point status which rapidly equals 2. The beam 1 slides continuously on the beam 2 from 0.25 s, except at the very beginning of the simulation, the normal and tangential contact component forces follows a time pattern without any discontinuities.

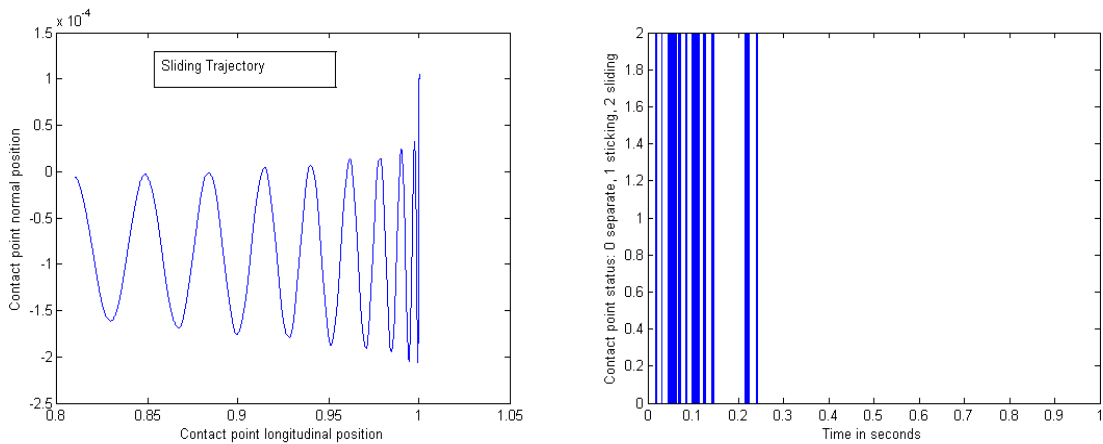


**Figure 2-3:** Contact point trajectory and contact point status in a stable case.

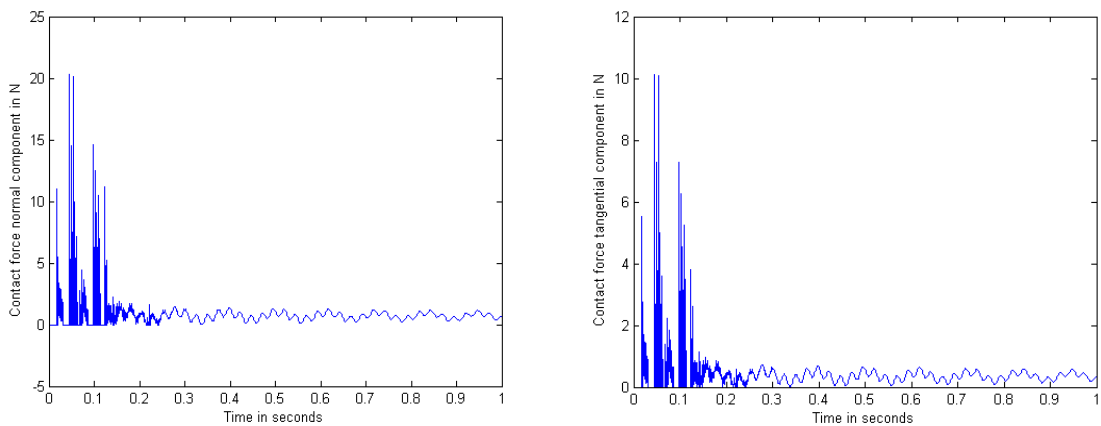


**Figure 4-5:** Contact point normal and tangential components in a stable case.

#### 3.2A first unstable case: a squealing case

We present in the following figures (6-7) and (8-9), an unstable case where the incident angle is still  $45^\circ$  and for the same external force applied in A, but the friction coefficient is raised to 1.5. As it can be seen the contact point trajectory exhibits periodic stops of roughly 0.07 seconds, corresponding to sticking phases followed by a mixed sliding-separate phase shorter. The contact force

patterns show periodic limit cycles corresponding to the appearance of an unstable mode. This limit cycle corresponds roughly to 900 Hz, what shows the zoom of the figure 10, where it can be seen how this unstable mode appears and disappears periodically, during roughly 0.02s. Consequently, this force will generate a non continuous squealing noise around 900 Hz, since the separation in between the apparition of these instabilities is sufficiently long (0.1 second) .

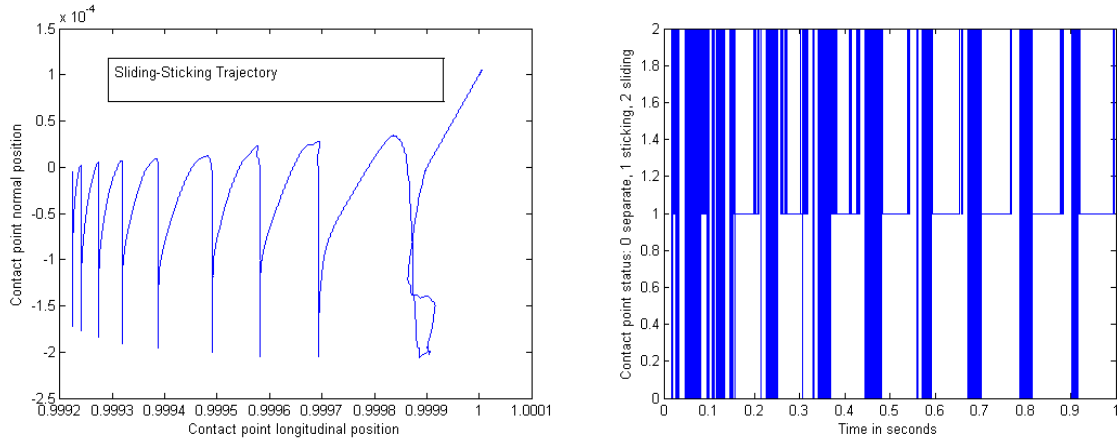


**Figure 6-7:** Contact point trajectory and contact point status in a squealing case.

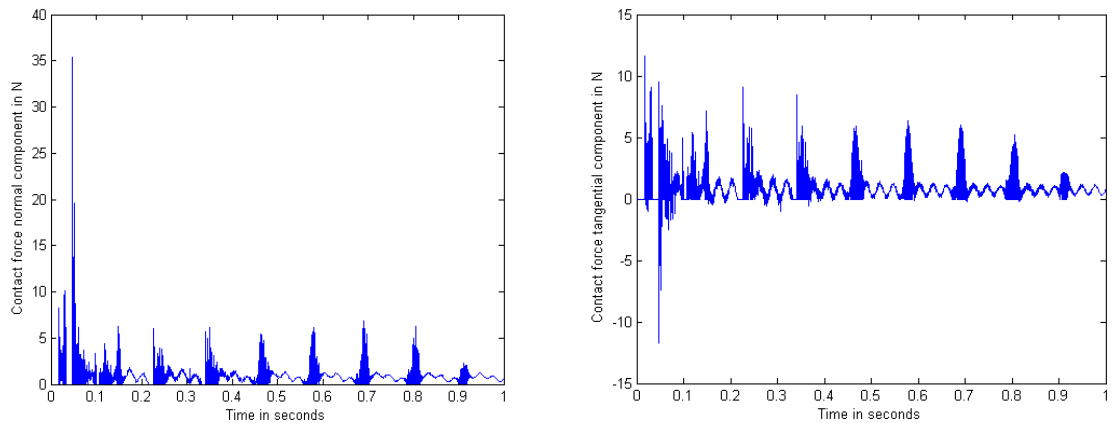


**Figure 8-9:** Contact point normal and tangential components in a squealing case.

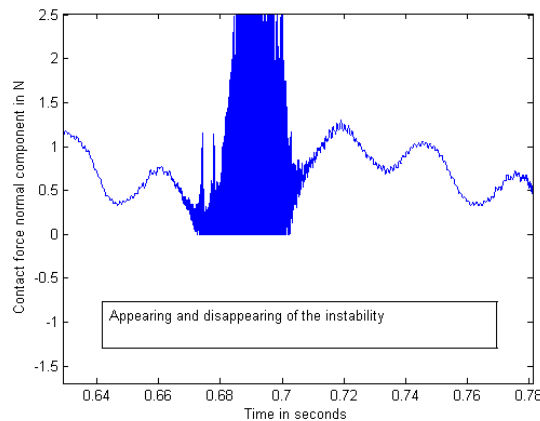


**Figure 10:** Appearance and disappearance of squealing noise around 900Hz.

### 3.3A second unstable case: a juddering case

To present a case of juddering, it consists in applying the constant force along the beam 1 principal axis as presented in figure (1). If the friction coefficient is smaller than unity, for an angle unchanged of 45°, the situation is stable and sliding as already shown in the figures (2-5). To render the system unstable the friction coefficient is raised to 1.1. As it can be seen, the system becomes unstable (figures (11-14)).

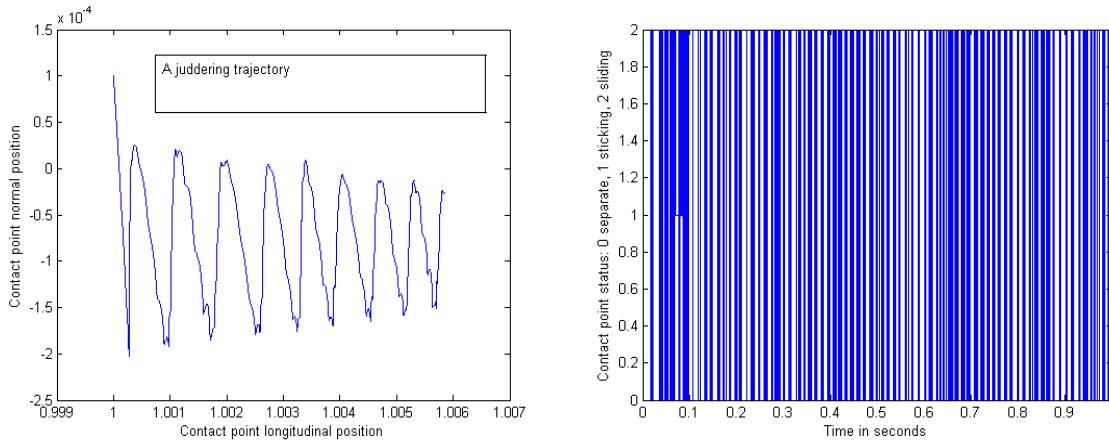


**Figure 11-12:** Contact point trajectory and contact point status in a juddering case.

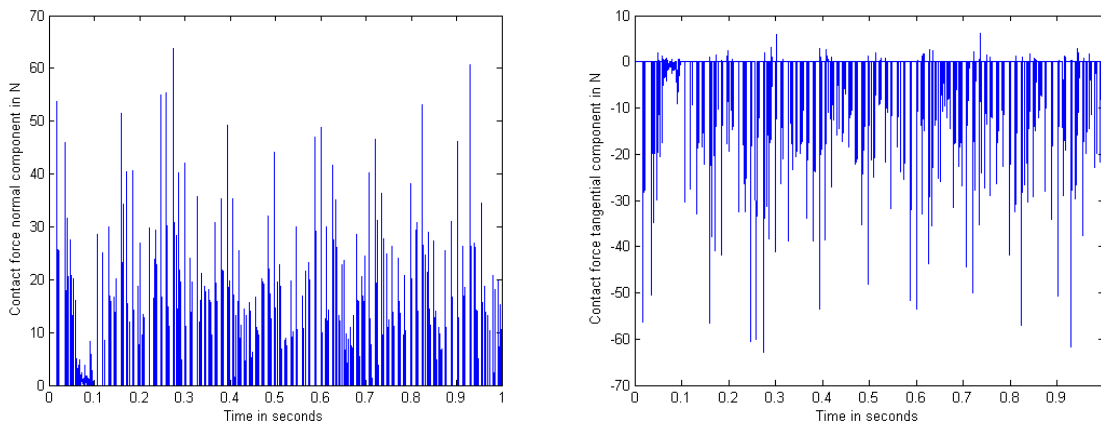


**Figure 13-14:** Contact point normal and tangential components in a juddering case.

The contact point status (figure (12)) varies a lot and never stabilizes. The contact forces are particular irregular and their values are highly spread (figure (13-14)). Namely separation are quite continuous (zero force value), and the peak values of the contact force are well higher than those encountered in the previous unstable case, meaning that this juddering unstable movement will generate a lot of vibration and radiated sound.

### 3.4 Excitation with an imposed velocity under constant pressure

Most of the time in a contact problem, a relative velocity in between the bodies interacting is known and a constant pressure is applied by external mechanical systems. The following figures are related to this problem where a constant velocity of 1 cm/s is imposed to the beam 1 in the direction paralleled to the beam 2. Moreover a constant vertical pressure normal to the beam 2 is imposed to the beam 1 at the point A. To cases of friction are simulated: the case of a weak pressure (2N) applied and a case of high pressure (50N). The constant friction coefficient is 1.2 and the relative

angle is  $-45^\circ$ . As can be seen, an unstable situation occurs in the case of the weak pressure (figures 15-16) looking like the juddering case already encountered. In figure 17, the central acceleration of the beam 2 at rest is presented, showing time patterns similar to the one of the normal contact force. This means that, as already mentioned, the time contact force patterns are sufficient to have an idea of the induced vibrations and consequently of the sound radiated.

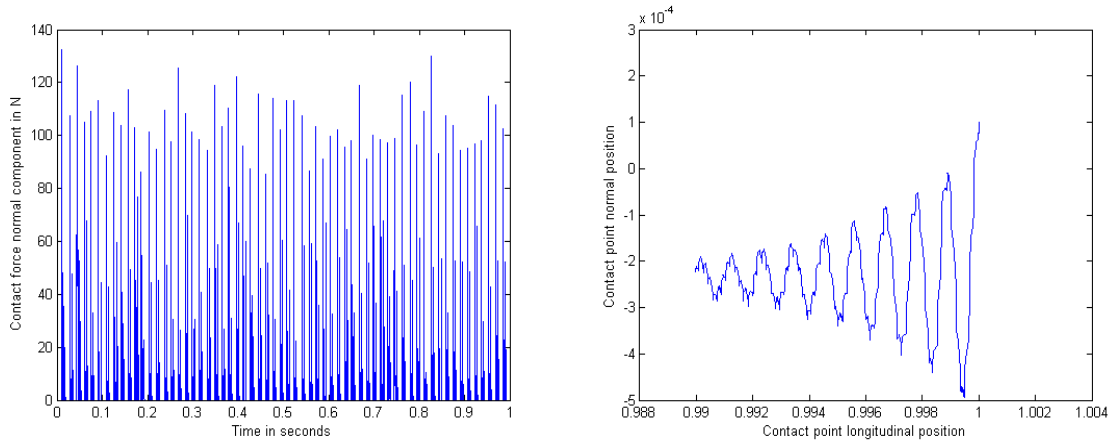


**Figure 15-16:** Contact point normal force and contact point trajectory for imposed velocity (1cm/s) and under weak constant pressure (2N).

When the pressure is high (50N) (figures (18-20)), this juddering situation is transformed into a squealing situation since the contact force patterns are totally changed into squealing patterns. Namely, sticking phases appears clearly and relaxation phases too. During these relaxation phases a high frequency unstable time pattern occurs at 2500Hz. Consequently the acceleration of the beam 2 exhibits the same time pattern and a corresponding squealing noise will be generated at 2500Hz. The contact point status shows that during the relaxation phases, that is to say when the beam 1 is not stocked to the beam 2, the contact point status switches rapidly from sliding to separate. It could also be shown that the higher the pressure the higher the squealing noise frequency.

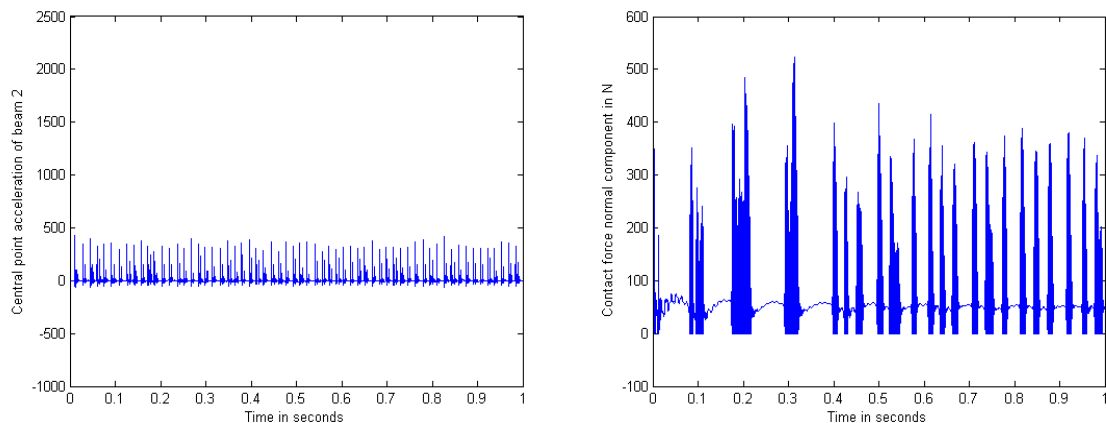


**Figure 17-18:** Beam2 central point acceleration for imposed velocity (1 cm/s) under weak pressure (2N) (left) and Contact point normal force for imposed velocity (1 cm/s) under high pressure (50N) (right).

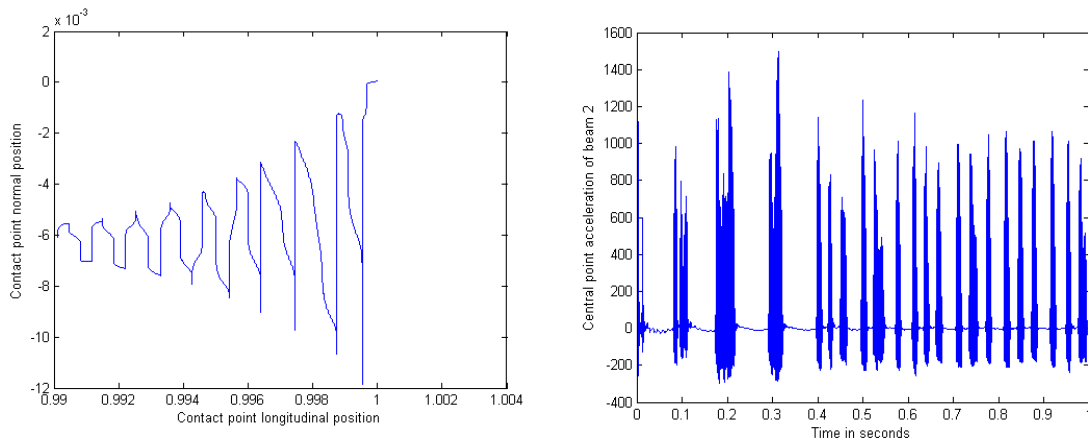


**Figure 19-20:** Contact point trajectory and beam 2 central point acceleration for imposed velocity (1cm/s) and under high pressure (50N).

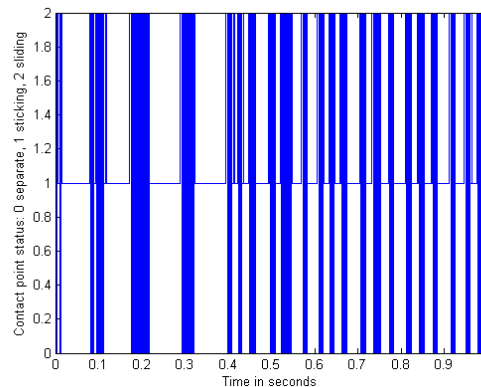


**Figure 21:** Contact point Status for imposed velocity (1cm/s) and under high pressure (50N)

## 4. Conclusion

We have shown that the use of a time modelisation of the friction noise allows us to predict reasonably the mains time pattern induced during instabilities. Depending on the friction coefficient value, the system becomes unstable and juddering or squealing appears. In the case where the velocity is imposed, the external pressure is a sensible parameter which, when raised, leads the system to change its instability mode: juddering for relative weak pressure and squealing for higher pressure.

## REFERENCES

- <sup>1</sup>. L. Baillet, S. D’Errico, B. Laulagnet, “Understanding the occurrence of squealing noise using the temporal finite element method”, *Journal of Sound and Vibration* **292**, 443-460 (2006).
- <sup>2</sup>. A. Meziane, S. D’Errico, L. Baillet, B. Laulagnet, “Instabilities generated in a pad-disc system during the braking process”, *Tribology International* **40(7)**, 1127-1136 (2007).